

## Active Docking of a Transport Cask Vehicle Subject to 6 Degrees of Freedom Misalignments\*

M. Isabel Ribeiro, Pedro Lima, Pedro Aparício, Renato Ferreira

Instituto Superior Técnico/ Instituto de Sistemas e Robótica,  
Av. Rovisco Pais 1, P-1096 Lisboa CODEX, PORTUGAL  
Tel: 351 1 8418059, Fax: 351 1 8418291, email: mir@isr.ist.utl.pt

**Abstract**—This paper presents a study on the docking of a mobile platform to a docking port where six degrees of freedom misalignments may occur in the general case. This study is motivated by a requirement of ITER, where mobile platforms are required for cask transference between the Vacuum Vessel and the Hot Cell Building.

### I. INTRODUCTION

This paper presents a study on the docking of a mobile platform to a docking port where six degrees of freedom (dof) misalignments (3 dof in position and 3 dof in orientation) may occur in the general case. This study is motivated by a requirement of ITER where mobile platforms are required for cask transference between the Vacuum Vessel Building (VVB) and the Hot Cell Building (HCB).

A common problem that arises when docking mobile platforms is the unavoidable existence of small position ( $x$  and  $y$ ) and orientation ( $yaw$ ) errors in the vicinity of the docking port. These small errors exist for any type of guidance solution used on the mobile platform to approach a docking station: optical or inductive steering in the case of a classical AGV platform, virtual path following if the reference path, defined as an on-line optimisation procedure, may be chosen along any free space of the environment, or mixed guided path if, on the later case, the mobile platform acts as a classical AGV in pre-specified zones of the operation environment. Additionally, as it happens on ITER, when docking at the VVB, the transport vehicle moves at the galleries while the docking port is in a different building structure, this yielding possible misalignments in  $z$ ,  $roll$  and  $pitch$ .

Two different procedures are required for precise docking: evaluation of the misalignments in the vicinity of the docking port and platform maneuvering aiming at decreasing them. In order to accomplish precise position and orientation relative to the docking port, a *laser* based system using retroreflectors for triangulation is suggested. The information provided by this system can be used by the transfer cask controller (e.g., a teleoperator) in order to minimize the number of maneuvers required to dock the mobile platform.

The main advantage of active docking over its passive counterpart is the possibility of remote assisted, *vs* local, hands-on operation. In the former, the localization infor-

mation may be complemented by suggestions to the operator on the required corrections. In the latter, passive compliance and contact between the cask and the docking port are requirements for the success of the docking operation.

### II. DOCKING

#### A. Notation and Frames

Fig. 1-a) shows a schematic representation of a cask approaching a docking port with only translation error along the  $y$  axis.

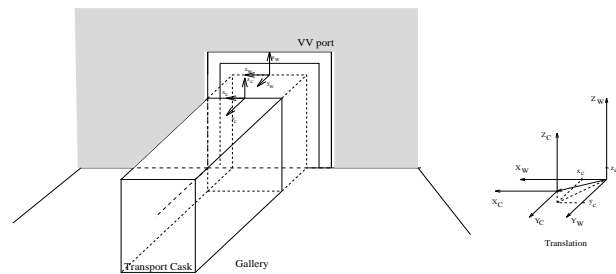


Fig. 1. a) Cask approaching docking port, b) Translation misalignment

In this figure there are two frames. One is linked to the cask  $\{C\}$  and the other,  $\{W\}$ , denoted as the world frame, is linked to the docking port. A cask is considered docked when the misalignment between the frames  $\{C\}$  and  $\{W\}$  is less than the threshold required for the subsequent remote handling operations to be fulfilled. In a precise docking the two frames exactly coincide.

In this particular problem, six degrees of freedom (dof) misalignments (3 dof in position and 3 dof in orientation) may occur in the general case. The 6 dof are represented by  $x$ ,  $y$ ,  $z$  for position, and by  $\gamma$  ( $roll$ ),  $\beta$  ( $pitch$ ) and  $\theta$  ( $yaw$ ) for orientation. Fig. 1-b) shows a schematic representation of the effect of buildings plus vehicle misalignment concerning position. Fig. 2 represents the contributions to the orientation misalignment that may exist between the two frames when no position error occurs and the corresponding scene (transport cask and VV port) is seen by someone in the gallery.

#### B. Sensor Description

The docking maneuvers are performed as a result of the knowledge of the translation and rotational misalignments between the transport cask and the docking port.

\* This work was done under the contract ERB 5004 CT 96 0127-NET/96-341 between the European Atomic Energy Community and the Association EURATOM/IST.

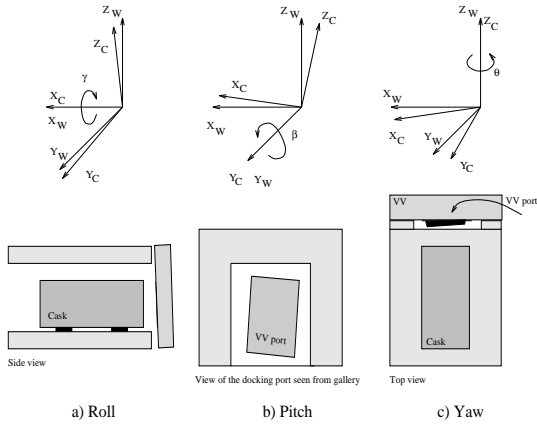


Fig. 2. Schematic representation of rotational misalignment and building misalignment seen from the gallery

To evaluate these misalignments, a sensorial system based on three laser scanners mounted on the cask and combined with passive retroreflectors properly installed on the docking port is proposed. A pre-processing of the raw data acquired by each laser scanner provides the angle with which each retroreflector is detected.

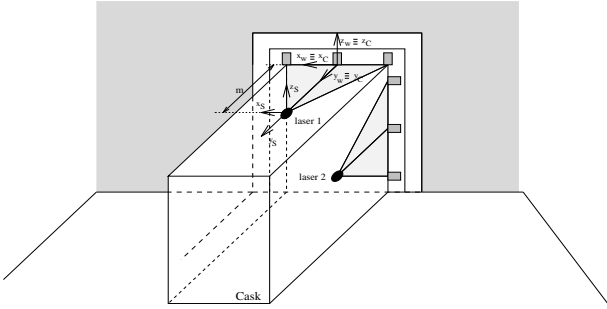


Fig. 3. Laser systems and associated frames in a precisely docked cask.

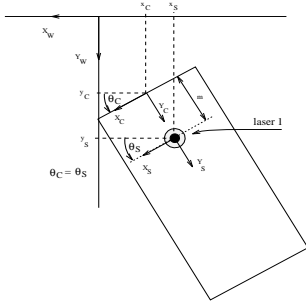


Fig. 4. Position and orientation on  $x - y$  plane.

The proposed *laser* system is used as follows: a *laser* sub-system is placed at the top of the vehicle (*laser*<sub>1</sub>). On the vehicle sides, two other *laser* sub-systems (*laser*<sub>2</sub> and *laser*<sub>3</sub>) are placed, one at each side, as illustrated in Fig. 3 where, for the sake of simplicity, *laser*<sub>3</sub> is not displayed. Due to technological limitations, a minimum distance between the *laser* diode and the retroreflector is imposed. Therefore, the *laser* sensors must to be placed some fixed

distance ( $m$ ) apart from the transfer cask border.

In the sequel, *laser*<sub>1</sub> is studied in detail. The study is directly applied to *laser*<sub>2</sub> and *laser*<sub>3</sub>. The frame associated with *laser*<sub>1</sub>, referred as  $\{S\}$  in Fig. 3, is related to the cask frame  $\{C\}$  by a translation  $m$  along  $Y_C$ . The coordinates of the origin of the frames  $\{S\}$  and  $\{C\}$ , expressed in  $\{W\}$ , are related by (1) as represented in Fig. 4.

$$\begin{aligned} \theta &= \theta_c = \theta_s \\ x_c &= x_s + m \cdot \sin(\theta) \\ y_c &= y_s - m \cdot \cos(\theta) \end{aligned} \quad (1)$$

### C. Triangulation

Triangulation is a mathematical procedure developed to evaluate position and orientation based on angles measured to points whose absolute location is known. In a 2D world, three angles are enough for absolute localization (position and orientation). This concept is widely used in mobile robotics, [2], and will be further detailed.

The proposed triangulation scheme is illustrated in Fig. 5. Measurements are done with a *laser* device that obtains

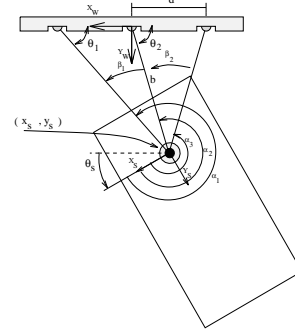


Fig. 5. Triangulation setup.

the angles,  $\alpha_1, \alpha_2, \alpha_3$ , with which three collinear retroreflective marks placed on previously known locations are detected. From the measured angles and the previously known distances between reflectors,  $d$ , position and orientation are unambiguously calculated as

$$x_s = -\frac{d}{\tan(\beta_1)} \cdot \frac{\tan(\theta_2) - \tan(\theta_1)}{1 + \tan^2(\theta_2)} \quad (2)$$

$$y_s = \frac{d}{\tan(\beta_2)} \cdot \frac{\tan(\theta_2) - \tan(\theta_1)}{1 + \tan^2(\theta_2)} \cdot \tan(\theta_2) \quad (3)$$

$$\theta_c = \theta_s = 2\pi - \alpha_1 - \theta_2 + \beta_1 \quad (4)$$

where,  $\beta_1 = \alpha_1 - \alpha_2$  and  $\beta_2 = \alpha_2 - \alpha_3$ .

The above equations yield the unambiguous computation of position ( $x_s$  and  $y_s$ ) and orientation ( $\theta_s$ ) of the  $\{S\}$  frame with respect to the  $\{W\}$  frame, in a 2D world, based only on three measured angles,  $\alpha_1, \alpha_2$  and  $\alpha_3$ . Note that the  $\{S\}$  frame and the  $\{C\}$  frame are related by a fixed transformation, (1), that does not depend on cask location relative to the world frame.

Equations (2) - (4) were derived in an ideal situation when no *roll* or *pitch* errors occur. In the particular docking problem under study, building misalignments will most likely introduce non null *roll* and/or *pitch* angles during the docking approach phase relative to the  $\{W\}$  frame. In that case, the errors readings will have some noise introduced by those rotations. Since the orientation errors are small (they reflect the buildings misalignments), the introduced noise will not have large amplitudes.

The lateral laser scanners,  $laser_2$  and  $laser_3$  yield the same type of information as a result of a triangulation procedure. Table I summarizes the information obtained by the three *laser* sub-systems, after processing the corresponding measurements.

Table I  
Information obtained from the *laser* sub-systems.

Sub-system	Information
$laser_1$	$x_s, y_s$ and $Yaw(\theta_s)$
$laser_2$	$y_2, z_2$ and $Roll_2(\gamma_2)$
$laser_3$	$y_3, z_3$ and $Roll_3(\gamma_3)$

The transport cask absolute orientation in terms of  $roll(\gamma_s)$ ,  $pitch(\beta_s)$  and position in terms of  $z_s$  can be evaluated from the combined information of  $laser_2$  and  $laser_3$  as follows, where  $CW$  represents the vehicle width.

$$z_s = \frac{z_2 + z_3}{2} \quad (5)$$

$$\beta_s = Pitch = \arcsin\left(\frac{z_2 - z_3}{CW}\right) \quad (6)$$

$$\gamma_s = Roll = \frac{\gamma_2 + \gamma_3}{2}, \quad (7)$$

Note that  $y_2$  and  $y_3$  might also be used to obtain a redundant evaluation of  $y_s$ .

#### D. Active Docking

The proposed docking procedure is implemented along the following lines: the transfer cask approaches the vicinity of the docking port in a fixed guidance mode. When in the near vicinity, and as soon as the laser sensors are able to detect the retroreflectors, the control is switched to a sensor-based mode. In fact, the vehicle can no longer follow the path defined in the gallery, since it will have to accurately dock to a VV port door and this door, being in a different building structure, may present misalignment in  $z$ , *roll* and *pitch*. In the sensor-based mode, the controller uses the knowledge of its location with respect to the VV docking door, to head towards this door.

The vehicle steering equipment can only correct the *yaw* angle,  $\theta$ , and the translational error in the  $x - y$  plane. Other strategies must be used to correct eventual misalignments in *roll*, *pitch* and in  $z$ . A possible solution is to use hydraulic actuators. With four hydraulic lifts in the vehicle, arranged in such a manner that they can change the container orientation (e.g., if placed in the corners), the *roll* and *pitch* effects can be corrected. With these actuators, the  $z$  component of the container can also be

corrected. Note that this type of solution can only correct small misalignments.

It is important to mention that final accuracy is also dependent on the resolution of the actuation systems used. This is a topic which deserves further study. Based on the localization information, the sequence of docking operations to be undertaken by a teleoperator, and the corresponding actuators, should be the following:

1. *roll* and *pitch* corrections by hydraulic actuators;
2.  $z$  corrections by hydraulic actuators;
3.  $x, y$  and *yaw* corrections by the steering/driving wheels.

### III. PERFORMANCE ANALYSIS

When using a triangulation scheme to measure position and orientation, a common source of error is noise in the measured angles. Therefore it is important to know how a small error in one, two and/or three of the measurements affect the estimated position and orientation. To evaluate the effects of those errors, simulations were made.

The graphics presented in Fig. 6 show the effects of errors in measurements of  $laser_1$  when the distance between reflectors,  $d$ , takes the values  $50cm$ ,  $100cm$  and  $150cm$  and  $\ell = 100cm$ . For each of these cases, two figures are presented, one for position and another for orientation, all of them being referred to the relations between the frames  $\{S\}$  and  $\{W\}$ . It was considered that the platform real position was such that the center of the  $laser_1$  is placed at  $x_s = 0$ ,  $y_s = \ell = 100cm$ ,  $\theta_s = 0^\circ$  with no *roll* or *pitch* errors. Then noise was added to angle measurements taken from that location. The amplitude of the introduced noise was calculated from the resolution presented in the specifications of a commercial *laser* system, [1]. In that system, the resolution is  $0.006^\circ$ . The introduced noise has  $0.024^\circ$  maximum amplitude being added in steps of  $0.006^\circ$  (four steps).

From Fig. 6 it is clear that absolute errors in position and orientation decrease when the distance between reflectors gets larger. Also, the errors in  $x_s$  are much reduced if distance between reflectors,  $d$ , is larger. Similar experiments were carried out for different values of  $\ell$ , [3]. The Table II summarizes the maximum deviations from the nominal values for  $x_s, y_s$  and  $\theta_s$ .

The summary of the simulations presented in Table II show that the placement of the *laser* sensor is extremely important for the global performance. It can be seen that the errors are greatly influenced by the distance,  $\ell$ , between the *laser* sensor and the reflectors wall. If the sensor is too far from the wall where the reflectors are placed, a small error in the measurement is amplified. On the other hand, if the sensor is too close there may be problems when the cask gets too close to the docking port because there is a minimum operation distance between the *laser* sensor and the retroreflective reflector. A typical minimum distance is 30 cm. Simulations have also shown

$y_s = 100$  centimeters.

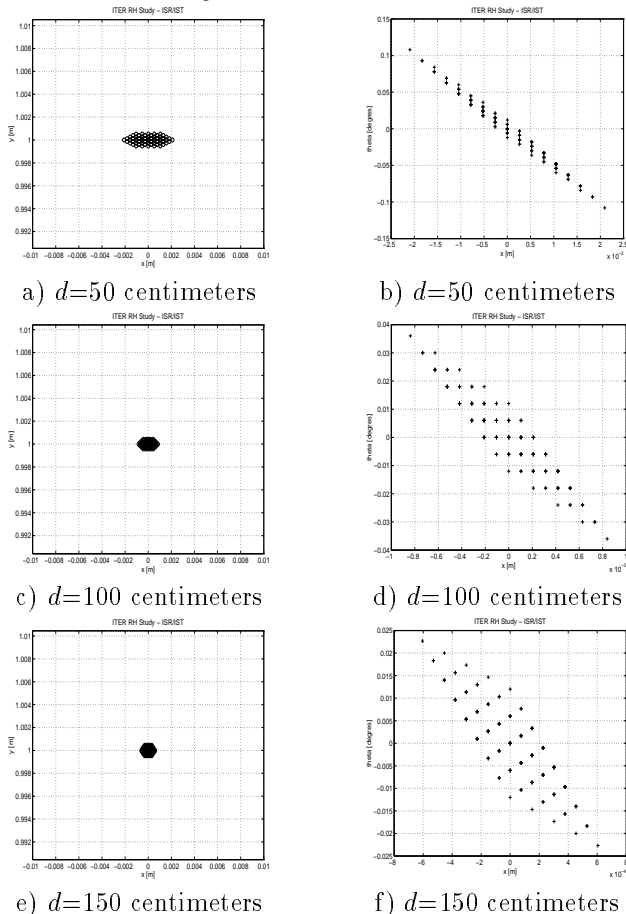


Fig. 6. Location errors due to errors on the detection of the reflector marks. Simulations made with sensor 100 cm from the wall.

that if the distance between reflectors is  $d = 150$  cm, a value between  $\ell = 50$  cm and  $\ell = 100$  cm is a good choice for sensor placement. This value has a good compromise distance/performance.

The results just presented refer to the location of the  $laser_1$  relative to the VV docking port, or, stated in a more formal way, of the location of the  $\{S\}$  frame relative to the  $\{W\}$  frame. As mentioned before, the vehicle frame  $\{C\}$  and the sensor frame  $\{S\}$  do not have coincident origins (See Fig. 4). Therefore, besides knowing the effects of small errors in position and orientation in the  $\{S\}$  frame, it is important to know their effect when propagated to the vehicle frame  $\{C\}$ . Only the effects of errors in one of the  $laser$  systems will be presented. For simplicity  $laser_1$  is used. For a nominal situation in which  $x_s = 0$ ,  $y_s = m$  and  $\theta_s = 0$  and assuming that  $\Delta x_s$ ,  $\Delta y_s$  and  $\Delta \theta_s$  are the errors in position and orientation yields,  $x_s = 0 + \Delta x_s$ ,  $y_s = m + \Delta y_s$ ,  $\theta_s = 0 + \Delta \theta_s$  which replaced in (1) and considering that the orientation deviation is small, *i.e.*,  $\cos(\Delta \theta) = 1$  and  $\sin(\Delta \theta) \simeq \Delta \theta$  leads to the errors on the  $\{C\}$  frame around the nominal

Table II

Comparative table on location errors

$\ell$ [m]	$d$ [m]	$x_s \pm \Delta x$ [m]	$y_s \pm \Delta y$ [m]	$\theta_s \pm \Delta \theta$ [degrees]
2.0	0.5	$0.0 \pm 0.0141$	$2.0 \pm 0.0018$	$0.0 \pm 0.396$
2.0	1.0	$0.0 \pm 0.0042$	$2.0 \pm 0.0010$	$0.0 \pm 0.108$
2.0	1.5	$0.0 \pm 0.0023$	$2.0 \pm 0.0009$	$0.0 \pm 0.054$
1.0	0.5	$0.0 \pm 0.0021$	$1.0 \pm 0.0005$	$0.0 \pm 0.108$
1.0	1.0	$0.0 \pm 0.0008$	$1.0 \pm 0.0004$	$0.0 \pm 0.036$
1.0	1.5	$0.0 \pm 0.0006$	$1.0 \pm 0.0005$	$0.0 \pm 0.022$
0.5	0.5	$0.0 \pm 0.0004$	$0.5 \pm 0.0002$	$0.0 \pm 0.036$
0.5	1.0	$0.0 \pm 0.0002$	$0.5 \pm 0.0003$	$0.0 \pm 0.018$
0.5	1.5	$0.0 \pm 0.0002$	$0.5 \pm 0.0003$	$0.0 \pm 0.014$

solution  $x_c = 0$ ,  $y_c = m$  and  $\theta_c = 0$ ,

$$\begin{cases} \Delta x_c = \Delta x_s + m \cdot \Delta \theta \\ \Delta y_c = \Delta y_s \\ \Delta \theta_c = \Delta \theta_s. \end{cases} \quad (8)$$

From equation (8) it is clear that small errors in  $\theta$  are amplified by a factor proportional to the distance  $m$  between the vehicle frame and the sensor frame.

As an example, considering  $m = 50$  cm and  $d = 150$  cm, the maximum  $\theta$  deviation is  $\theta = 0.014^\circ$ . From equation (8) and the data presented in Table II, yields

$$\begin{cases} \Delta \theta_c = \pm 0.014^\circ \\ \Delta x_c = 0.0002 + 0.5 \cdot 0.014 \cdot \frac{\pi}{180} \simeq 0.0004[\text{cm}] \\ \Delta y_c = 0.0003[\text{cm}] \end{cases} \quad (9)$$

#### IV. CONCLUSIONS

In this paper we proposed an active solution for the ITER transport cask docking problem, based on three rotating laser systems located on the casks and nine retroreflectors located on the docking port. The complete system is capable of providing to a teleoperator the position and orientation of the cask with respect to the VV docking port based on a triangulation method.

The localization errors were quantified based on the resolution of a typical commercial rotating laser system associated to three retroreflectors. Simulations for different distances between collinear retroreflectors and distances between the three retroreflectors and the emitting laser, led to the conclusion that it is possible to design such a system to assist the teleoperator with localization errors within ITER specifications for docking ( $\pm 5$  mm).

#### REFERENCES

- [1] H.R.Everett, *Sensors for mobile Robots: Theory and Applications*, A K Peters, Ltd.
- [2] P.J.McKerrow, *Introduction to Robotics*, Addison Wesley Publishing Company, 1991.
- [3] M.I.Ribeiro, P.Lima, P.Aparício, R.Ferreira, *Conceptual Study on Flexible Guidance, Navigation and Docking Systems for ITER RH Transport Casks*, Technical Report ISR-403-97, Instituto de Sistemas e Robótica, Instituto Superior Técnico, April 1997.